

WAKE FIELDS EVALUATION FOR BEAM COLLIMATORS AND THE 60 PC ELECTRON BEAM AT THE COMPACT ERL AT KEK*

O. A. Tanaka[†], N. Nakamura, T. Obina, Y. Tanimoto, T. Miyajima, M. Shimada, High Energy Accelerator Research Organization, KEK, Tsukuba, Japan
N. P. Norvell, SLAC National Accelerator Laboratory, Menlo Park, USA

Abstract

In high-intensity particle accelerators, unwanted transverse and longitudinal wakefields arise when the high-charge particle beam passes through the narrow chambers or locations with small transverse apertures, such as collimator jaws. The transverse wake field may affect the beam emittance and the longitudinal wake field can cause the energy loss and the energy spread. In the present study we investigated the collimator's impact to the beam performance. In this paper, we have shown numerical, analytical and measurement results on the collimator's wakefields that will be important for the next step operation. Thus, considering future cERL upgrade to the IR-FEL, a possibility of consequent degradation of the FEL performance should be taken into account. The correspondent power loss was obtained as 13.7 W (81.25 MHz, 5 mA, 2 ps).

INTRODUCTION

The Compact ERL (cERL) at KEK [1] has five collimators (one in the injector section, one in the merger section and three in the recirculation loop, see Fig. 1) to remove the beam halo and to localize the beam loss. An operation at 10 mA average beam current and 1.3 GHz repetition rate is planned in the near future. The collimator's wakefields are expected to play an important role in CW operation, when the bunch charge will be increased up to 80 pC. The current beam parameters of the cERL are summarized in the Table 1.

All cERL collimators consist of four cylindrical rods of 7 mm radius made from copper. They could be independently inserted from the top, bottom, left and right sides of the beam chamber. Collimators COL1 – 3 were designed for the straight sections, therefore they have a round chamber 50~mm radius made from stainless steel. Its schematic is given at Fig. 2.a. Note that the beam energy at collimators COL1 – 2 is 2.9 MeV, while the energy at the rest of them is 17.6 MeV. Collimators COL4 – 5 are dedicated to the arc section, thus their chambers have elliptical shape with 70x40~mm diameter. Materials used are the same. The detailed scheme can be found at Fig. 2.b.

In the present study, first, we have estimated the transverse kicks imposed by the collimator's rods. This calculation is needed to account for the beam blow up (emittance growth) associated with collimator's wake. Then, the longitudinal wakes are calculated to obtain the expected energy losses of the beam passing through the collimator and its energy spread. Finally, those results are compared with the beam measurements in cERL. The present study is necessary towards the IR-FEL upgrade of cERL [2 – 3].

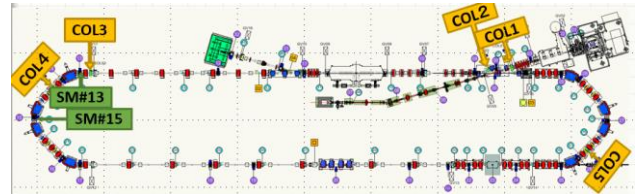


Figure 1: Layout of the cERL and its collimators.

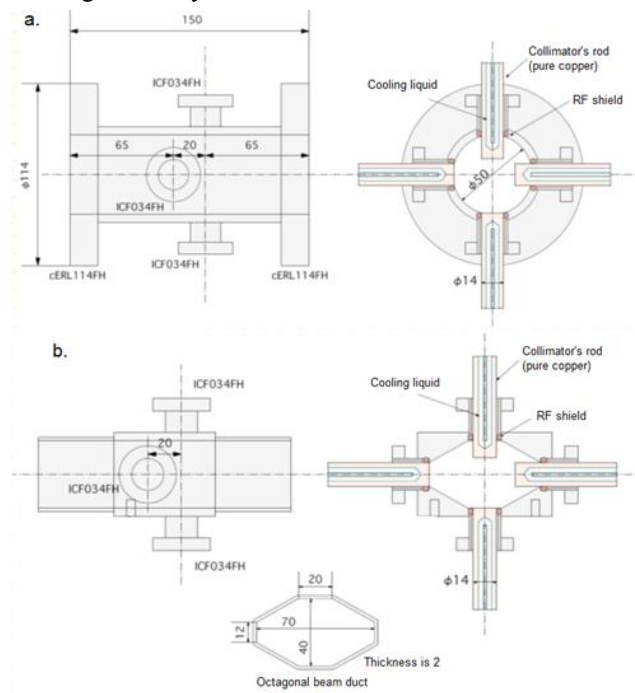


Figure 2: Schematic of the collimators with chambers made of stainless steel and rods made of copper: a. Collimators COL 1 – 3 for the straight sections; b. Collimators COL 4 – 5 for the arc sections.

Table 1: cERL electron beam parameters

Parameter	Design	In operation
Beam energy [MeV]:		
Injector	2.9	2.9
Recirculation loop	18	17.6
Bunch charge [pC]	60	60
Repetition rate [GHz]	1.3	1.3
Bunch length (rms) [ps]	2	Under tuning
Energy spread [%]	0.088	Under tuning
Normalized emittance (rms) in injector $\gamma\epsilon_x, \gamma\epsilon_y$ [$\mu\text{m}\cdot\text{rad}$]	1, 1	Under tuning

[†] olga@post.kek.jp.

TRANSVERSE WAKES AND EMITTANCE GROWTH

Let us consider transverse wakefields created by the vertical rods of the collimator. The simplified scheme of the collimator is demonstrated at Fig. 3. Here the vacuum duct's half aperture is $b = 25$ mm. The collimator's half gap is $a = [0; 25]$ mm. There is no tapers, so that the taper angle is $\alpha = \pi/2$. The rod's length is $L = 14$ mm. The value y_0 denotes the beam offset. The longitudinal beam distribution $\lambda(s)$ considered to be Gaussian.

For the geometry given at Fig. 3 in the beam near-axis approximation, when the dipole kick is applied to the centroid of the bunch, one can write down the dipolar mode of the *geometric component* of the transverse wake kick factor as follows [4]:

$$k_g = \frac{Z_0 c}{4\pi} \left(\frac{1}{a^2} - \frac{1}{b^2} \right) \quad \text{for} \quad \sqrt{\frac{\alpha a}{\sigma_z}} > 0.37. \quad (1)$$

Here we consider the collimator to be in purely diffractive regime [5]. In Eq. (1) the value $Z_0 = 120\pi$ is the impedance of the free space, $c = 2.9979 \times 10^8$ m/s is the speed of light, and $\sigma_z = 0.6$ mm is the rms bunch length.

Then, the *resistive component* of the collimator wake kick factor was evaluated with [6]:

$$k_r = \frac{\pi}{8a^2} \Gamma\left(\frac{1}{4}\right) \sqrt{\frac{2}{\sigma_z \sigma_z Z_0}} \left(\frac{L}{a} + \frac{1}{\alpha} \right). \quad (2)$$

Note that Eq. (2) refers to the so-called ‘‘long collimator’’ regime [7] that is exactly our case. Thus, the condition $0.63(2a^2 / Z_0 \sigma)^{1/3} \ll \sigma_z \ll 2a^2 Z_0 \sigma$ is satisfied. The value $\Gamma(1/4) = 3.6265$, while $\sigma = 5.96 \times 10^7$ S/m is the electrical conductivity of copper.

The CST Particle Studio [8] was used for the wakefields simulations. The 3D models of the collimators are shown in Fig. 4. Since the differences coming from the various chamber geometries was found to be negligible, we focused for simplicity on the circular one. Six million hexahedral meshes were set for the simulation. The half gap a was scanned from 0.1 mm up to 1.5 mm. The dipolar impact was calculated by setting the integration path to $y = 0$. The quadrupolar impact is calculated by setting the integration path to $y_0 = 0.05$ and 0.2 mm. A direct integration method was used.

The summary of simulation results together with analytical calculations is demonstrated at Fig. 5. The analytical curve for the geometrical component (blue line) is several orders bigger than those for the resistive-wall component (magenta line). Therefore, the total kick graph (red line) almost coincides with those for the geometrical component (blue line). The results of the corresponding CST simulations for the beam offsets $y_0 = 0.05$ mm (triangle) and $y_0 = 0.2$ mm (circles) are also shown in Fig. 5 and are in very good agreement with the analytical calculations. The resistive-wall component is small due to relatively short

length of the collimator (14 mm). The geometrical component is slightly bigger due to the absence of tapers in the collimator's design.

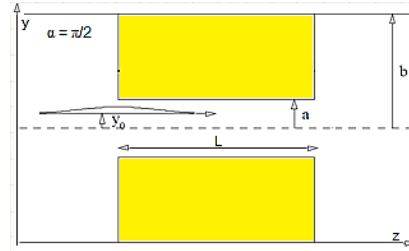


Figure 3: Simplified scheme of the collimator.

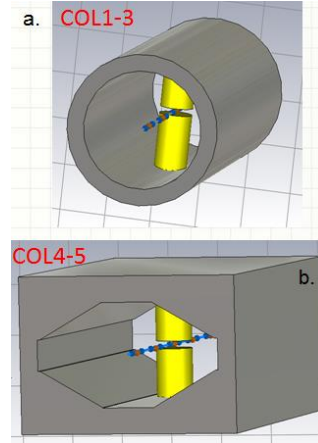


Figure 4: CST 3D models of the collimators with chambers made of stainless steel and rods made of copper: a. Collimators COL 1 – 3 for the straight sections; b. Collimators COL 4 – 5 for the arc sections.

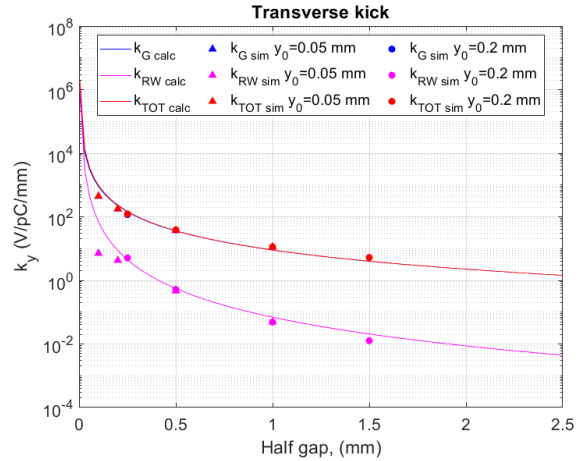


Figure 5: Transverse wake kick factors of the collimators found from analytical calculations and CST simulations for the geometrical and resistive wall component and different beam offsets.

The emittance blow-up for the 60 pC electron bunch at cERL was estimated. To account for this effect, the following analytical expression was treated [9]:

$$\frac{\Delta \varepsilon_y}{\varepsilon_{y0}} = \sqrt{1 + \frac{\beta_y \sigma_\omega^2}{\varepsilon_{y0}}} - 1, \quad (3)$$

where the value $\Delta\varepsilon_y$ is the *transverse emittance growth* with respect to the initial emittance ε_{y0} . The rms of the centroid kicks caused by the longitudinally varying field σ_ω could be found as follows [10]:

$$\sigma_\omega = \frac{Q}{E/e} k_\perp^{rms} y_0. \quad (4)$$

The value E is the beam energy at the location of collimator (see Table 1). The value $Q = 60$ pC is the bunch charge. The value y_0 is the beam centroid offset (see Fig. 3), and lastly, the value k_\perp^{rms} is the rms kick factor, estimated for the bunch head-tail difference in the kick. For Gaussian bunch $k_\perp^{rms} = k_\perp/\sqrt{3}$.

The resulted emittance blow-up found from Eq (3) are summarized in Table 2. The values of the initial emittances and beta functions at all locations are design values outputted from the tracking codes (General Particle Tracer [11] for the injector, and Strategic Accelerator Design for the recirculation loop [12]). The value of the transverse kick k_\perp is taken with respect to the collimator half gap $a = 1.5$ mm, and the beam centroid offsets $y_0 = 0.05$ mm and 0.2 mm. The emittance growth was found to be of the order of one percent or less.

Table 2: Expected values of the emittance blow-up for the collimator half gap 1.5 mm

Collimator	ε_{y0} [$\mu\text{m}\times\text{rad}$]	β_y [m]	$\Delta\varepsilon_y/\varepsilon_{y0}$ [%]
COL1 E=4 MeV	1.15	27.47	1.05
COL2 E=4 MeV	1.25	19.23	0.84
COL3 E=17.6 MeV	0.954	34.76	3.82
COL4 E=17.6 MeV	0.954	6.99	1.61
COL5 E=17.6 MeV	0.954	6.99	1.61

LONGITUDINAL WAKES AND ENERGY SPREAD

Now let us consider the longitudinal wake fields excited by the particles passing through the collimators. The values of the wake-loss factor were evaluated numerically through CST simulation for half-gap values in the range of 0.1 to 1.5 mm. The dependence of the energy spread on the collimator's half gap for the designed (2 ps) and current (4.5 ps) bunch length is demonstrated at Fig. 6.

For the analytical description, the following equation was used [13]:

$$k_{||} = \frac{Z_0 c}{2\pi^{3/2} \sigma_z} \ln\left(\frac{b}{a}\right), \quad (5)$$

where the value $Z_0=120\pi$ is the impedance of the free space, c is the speed of light, σ_z is the bunch length, $b = 25$ mm is the vacuum duct's half aperture, and a is the collimator's half gap.

The energy loss of the bunch at one collimator for the 60 pC per bunch burst mode with bunch length 2 ps, and collimator half gap $a=1.5$ mm:

$$\Delta E = k_{||} Q^2 = 46.86V / pC \times (60 pC)^2 = 168.7 nJ. \quad (4)$$

The voltage received by the electrons is $\Delta V=k_{||}\times Q=2812$ V. The energy of one electron is reduced by $e\Delta V=2812$ eV. If $E=17.6$ MeV, and since $E=17.6$ MeV, the relative energy

change is $e\Delta V/E=0.016\%$. For Gaussian bunch the energy spread due to one collimator is $\sigma E=0.4\times k_{||}\times Q=1124V$. With respect to the beam energy the wake-induced energy spread reads $\sigma E/E=0.0063\%$. Unfortunately estimated values are beyond the limits of the resolution of our monitors, and we could not detect them.

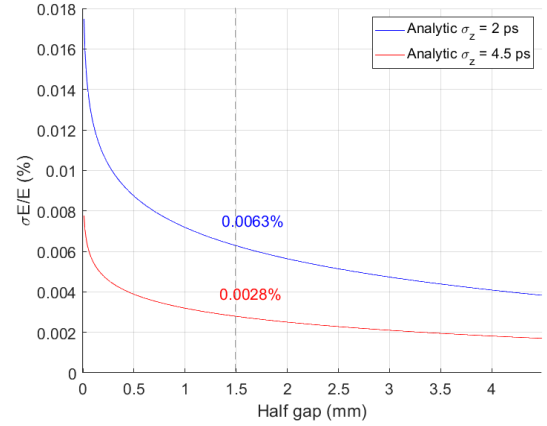


Figure 6: Wake-induced energy spread for different values of the collimator half gap and bunch lengths 2 ps (blue line) and 4.5 ps (red line).

BEAM-BASED MEASUREMENTS

For the measurement of the energy spread caused by the collimator's longitudinal wake, we used collimator COL3 located in the end of the north straight section, screen monitor SM#13 located between collimator COL3 and the entrance of the arc section, and screen monitor SM#15 located just in the middle of the arc (see Fig. 1). The screen monitor SM#13 needed to monitor the beam spot, which was successively cut by collimator's rods. The measurement itself was done by the screen monitor SM#15. To do so, first, we have restored the history of the quadrupole magnets to have the best beam spot at the collimator COL3 location. Then we have degaussed all quadrupoles of the first arc between screen monitors SM#13 and SM#15 to maximize the dispersion. We have measured the dispersion to be 2.41 m. The default energy spread was $\sigma E/E_{\text{default}}=\sigma_x/\eta=0.117\%$. It is the ratio of the rms beam size to the dispersion. However, in the following we care only on the changes of the energy spread and not on its absolute value.

The next step was to insert the collimator COL3. We used two horizontal rods, because the beam spot at the collimator location is known for its vertical beam halo. Therefore, we have avoided an influence of the halo on our energy spread measurement. We have performed the measurement for the half gap values 2 mm, 1.5 mm, 2 mm, 2.5 mm, 4 mm, COL out accordingly. Related rms beam sizes and beam profile peak positions were recorded at the screen monitor SM#15. The raw data of the beam profile was fitted by Gaussian fitting routine and weight analysis. An example on how the measured data were processed are shown in Fig. 7. Here the upper image is a SM#15 beam spot, the blue curve at the bottom plot is the raw data, the red line is its Gaussian fit, and the magenta mark denotes the peak position with respect to the data weight.

Weight analysis [14] gives the following expression for the profile peak position:

$$x_c = \frac{1}{N} \sum_{i=1}^{659} x_i N_i, \quad N = \sum_{i=1}^{659} N_i. \quad (6)$$

Here N is the number of data points, and x_i is the value of the i^{th} data point. The rms beam size is given by:

$$\sigma_x = \sqrt{\frac{1}{N} \sum_{i=1}^{659} N_i (x_i - x_c)^2}. \quad (7)$$

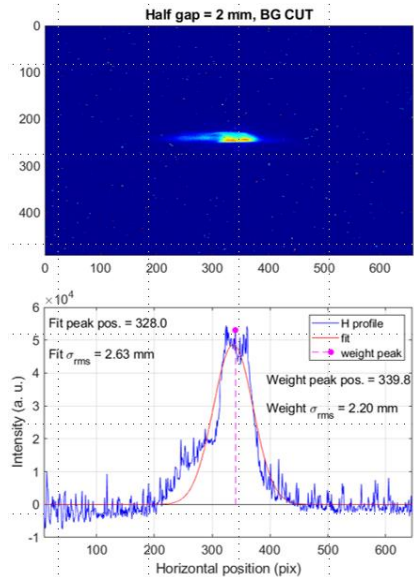


Figure 7: Energy spread measurement data at the screen monitor SM#15: the beam spot (top), the raw data and its fit (bottom).

Results of the processing of all six measurements are demonstrated at Fig. 8. The rms beam size is not changed significantly within the error bar except in the case of the 1.5 mm half gap. It was predicted by simulation and calculation. The beam size drop at the half gap 1.5 mm indicates that the beam core was damaged by the collimator's rod.

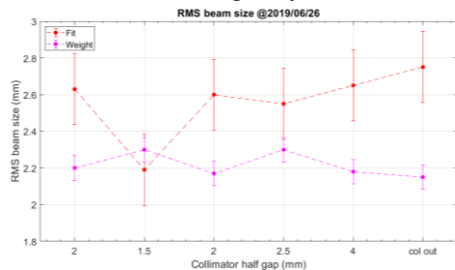


Figure 8: Horizontal beam size at the screen monitor SM#15 with respect to the horizontal collimation: fitting result (red), weight analysis result (magenta).

CONCLUSION AND OUTLOOK

The effect of the collimator's transverse and longitudinal wakes on the 60 pC electron beam performance was studied. It should be taken into account for an intense short bunch, when a considerable beam collimation is required. We have estimated the expected emittance growth due to collimator's wake field under the current operational conditions at cERL to be a few percent or less. The additional

energy spread due to collimator's wake at cERL is found to be 0.0028 % at 17.5 MeV, which is negligibly small.

Experimentally we have found, that for the current beam parameters even with the collimator's half gap at 2mm, the emittance and energy spread are not considerably affected. Thus the beam collimation at cERL was approved.

Considering the future cERL upgrade to the IR-FEL, the possibility of a consequent degradation of the FEL performance should be taken into account. The estimated power loss of 13.7 W was obtained for 81.25 MHz, 5 mA, 2 ps.

ACKNOWLEDGEMENTS

This research is carried out with the support of NEDO project "Development of next generation laser technology with high brightness and high efficiency".

REFERENCES

- [1] R. Kato, *et al.*, "Current status of KEK Compact ERL", in *Proceedings of the 16th Annual Meeting of Particle Accelerator Society of Japan*, Kyoto, Japan, (in press).
- [2] R. Kato *et al.*, "Development of high repetition middle infrared free electron laser using cERL", in *Proceedings of the 16th Annual Meeting of Particle Accelerator Society of Japan*, Kyoto, Japan, (in press).
- [3] O. Tanaka *et al.*, "High bunch charge operation of cERL for infrared free electron laser test", in *Proceedings of the 16th Annual Meeting of Particle Accelerator Society of Japan*, Kyoto, Japan, (in press).
- [4] G.V. Stupakov, "High-Frequency Impedance of Small-Angle Collimators", in *Proc. of 2001 Particle Accelerator Conf. (PAC01)*, Chicago, USA, June. 2001, pp. 1859-1861.
- [5] M. Dohlus, I. Zagorodnov, O. Zagorodnova, "Impedances of Collimators in European XFEL", TESLA-FEL Report 2010-04, July 2010.
- [6] P. Tenenbaum, "Collimator Wakefield Calculations for ILC-TRC Report", LCCNOTE-0101, 2002.
- [7] I. Zagorodnov and K.L.F. Bane, "Wakefield calculations for 3D collimators", in *Proc. of 10th European Particle Accelerator Conference (EPAC 2006)*, Edinburgh, UK, June. 2006, pp. 2859 – 2861.
- [8] CST-Computer Simulation Technology, CST PARTICLE STUDIO, <http://www.cst.com/Content/Products/PS/Overview.aspx>.
- [9] M. Dohlus, T. Limberg, "Impact of Optics on CSR-Related Emittance Growth in Bunch Compressor Chicanes", in *Proc. of 21st Particle Accelerator Conference (PAC05)*, Knoxville, USA, May. 2005.
- [10] S. Di Mitri, *PhysRevSTAB* 13,052801 (2010).
- [11] GPT - A simulation tool for the design of accelerators and beam lines, <http://www.pulsar.nl/gp>.
- [12] Strategic accelerator design, <http://acc-physics.kek.jp/SAD>.
- [13] S. Heifets and S. Kheifets, "Coupling impedance in modern accelerators", *Rev. Mod. Phys.* vol. 63, p. 631, Jul. 1991. doi:10.1103/RevModPhys.63.631
- [14] P. R. Bevington and D. K. Robinson, *Data Reduction and Error Analysis for the Physical Sciences*, McGraw-Hill, 1992.